

**Pattern Formation driven
by Transport, Drift,
and Localized Interactions**

Angela Stevens

University of Münster

[Scheel - S.]

We study mechanisms for wavenumber selection in a minimal model for run-and-tumble dynamics.

$$\begin{aligned}u_t &= +u_x - r(u, v) + r(v, u), \\v_t &= -v_x + r(u, v) - r(v, u).\end{aligned}$$

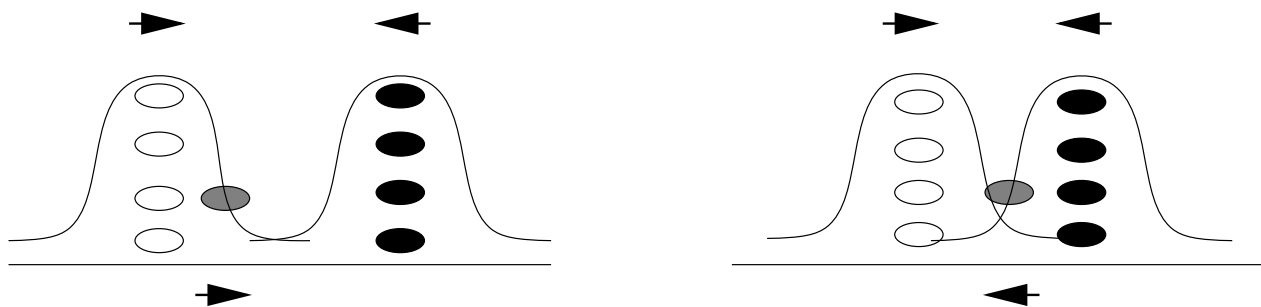
The nonlinearity r in tumbling rates induces the existence of a plethora of traveling- and standing-wave patterns, as well as a subtle selection mechanism for the wavenumbers of spatio-temporally periodic waves.

Example: Rippling in populations of myxobacteria.

The ripple crests are oriented approximately perpendicular to the movement direction of the bacteria.

A cell-surface bound C-signal is transmitted upon end-to-end contact, of individual bacteria and increases their reversal probability.

Bacteria move with the same speed to either right or left.
They may change orientation, and move in the opposite direction.
Let the tumbling events be pointwise functions of the two densities,
thus encoding the probabilities of encounters between
left- and right-moving bacteria.



Inspired by Turing the most accessible scenario for pattern formation in diffusion-reaction systems is the instability of an unpatterned, spatially homogeneous state against perturbations with spatial structure.

The linearly fastest growing mode then allows for rough predictions of wavenumbers in nonlinear systems.

Notice: absence of diffusion in one species out of two, does **not** lead to selection of finite wavenumbers in linear instabilities

But patterns with well-defined wavenumber laws have been experimentally observed in such situations (Liesegang rings).

Our caricature example reads

$$\begin{aligned}u_t &= +u_x - r(u, v) + r(v, u), \\v_t &= -v_x + r(u, v) - r(v, u).\end{aligned}\tag{1}$$

$u = u(t, x)$, $v = v(t, x)$ encode the densities of left- and right-moving bacteria.

$r(u, v)$ is the rate at which left-moving bacteria reverse direction.

Such systems do arise as special lower dimensional cases from structured population dynamics models

$$\partial_t U(t, x, c) + V(c) \cdot \partial_x U(t, x, c) + \partial_c [K(U(t, x, c))] = 0.\tag{2}$$

Here $\{c\}$ denotes a set of internal (state) variables, i.e. the direction of motion.

The most distinctive feature of the operator K is, that it acts on the density U in a local manner.

Classification of pattern formation in such systems is largely open.

For simplicity we focus in our analysis on

$$r(u, v) = u \cdot g(v), \quad g(v) = 1 + \frac{v^2}{1 + \gamma v^2}, \quad (3)$$

for $\gamma \geq 0$.

Here $g(v) \equiv 1$ encode spontaneous tumbling,

linear dependence $g(v) = v$ encodes binary collisions,

albeit with zero net effect on the dynamics due to the presence of the reverse tumbling, $ug(v) - vg(u) = 0$.

We keep the next simplest term $g(v) = v^2$, encoding triple collisions, and we also allow for a Hill-type saturation of the tumbling rate for large densities through the denominator $1 + \gamma v^2$.

The interaction of tumbling and transport appears to be surprisingly difficult to characterize.

Systems (1) exhibits spatially constant equilibrium densities when $r(u, v) = r(v, u)$, which is satisfied for $u \equiv v$ (*symmetric states*), but possibly also along curves where $u \neq v$ (*asymmetric states*).

The linearization at symmetric states does **not** predict finite wavelength patterns as fastest growing modes of the linearization.

At the onset of instability, **all** spatial wavenumbers become simultaneously naturally stable, with EVs on the imaginary axis.

Past onset spatially homogeneous perturbations exhibit the fastest growth rate.

“Turing instabilities”, where the first instability occurs for a wavenumber $0 < k_* < \infty$, arise only when more complexity is allowed, e.g. different stages of right and left moving bacteria, u_j, v_j , $j \geq 2$, [Primi-S.-Velazquez, S.-Velazquez].

Our main results here can be informally summarized as follows:

1. *linear growth favors wavenumbers $k_{\text{lin}} = 0$ or $k_{\text{lin}} = \infty$, that is, linear instabilities **do not select** finite wavenumbers from white-noise perturbations;*
2. *localized perturbations of asymmetric states may generate traveling waves with a selected non-zero wavenumber k_{loc} , that is, instabilities **do select** finite wavenumbers from shot-noise perturbations;*
3. *localized perturbations of symmetric states result in the creation of asymmetric states and subsequent evolution of traveling and standing waves, with nonzero wavenumber k_{loc} , that is, localized instabilities **eventually do select** finite wavenumbers from shot noise perturbations.*

Localized perturbations result in their spatio-temporal **spreading**.

The emerging invasion process is oscillatory in nature with a well-defined spreading speed and finite temporal frequency.

In other words, **oscillatory invasion selects spatial wavenumbers**.

These selection mechanisms are not induced by diffusion.

Indeed, linear growth from white noise may favor a finite wavenumber $0 < k(\varepsilon) < \infty$ in the related model with diffusion, but $k(\varepsilon) \rightarrow 0$ or $k(\varepsilon) \rightarrow \infty$ for $\varepsilon \rightarrow 0$, for these perturbations.

For shot noise perturbations, diffusion plays a subordinate role, and the selected wavenumber $k_{\text{loc}}(\varepsilon)$ is continuous in ε with nonzero limit at $\varepsilon = 0$.

Dynamics of pure tumbling kinetics in the phase plane for r as in

(3) with $\gamma = 0.122, 0.115, 0.07, 0.021$

Stability changes correspond to horizontal tangencies
of curves of equilibria.

Wavenumber selection from localized perturbations of symmetric states.

Alignment:

$$\begin{aligned}\partial_t f(t, \gamma) &= - \int_I T[f](\gamma, \gamma') f(t, \gamma) d\gamma' \\ &\quad + \int_I T[f](\gamma', \gamma) f(t, \gamma') d\gamma'\end{aligned}$$

where $T[f](\gamma, \gamma') = \int_I G_\sigma(\gamma' - \gamma - V(w - \gamma)) f(t, w) dw$,
 $I = [-\frac{1}{2}, \frac{1}{2}]$, V is the orientational angle,

an odd function and 1-periodic,

G_σ measures the accuracy of reorientation

and can be chosen as the standard periodic Gaussian.

Bi-Directional Alignment - Attraction and Repulsion:

If the angle between myxobacteria is small, they attract each other.

If the angle between myxobacteria is larger, they are repulsive, respectively they are attracted to the ends of their interaction partners.

Peak Solutions for the Limiting Equation:

Consider G_σ with $\sigma = 0$, the Dirac mass δ_0 , which describes deterministic turning.

Convergence of solutions of our equation for G_σ to solutions for δ_0 , for σ small enough, was proved by E. Geigant.

[Kang - Perthame - S. - Velázquez]

For continuously varying initial distributions
an exchange of mass and generalized momenta takes place.

Define suitable partial masses $m_1(t), m_2(t)$ as well as
suitable means of partial first moments $\xi_1(t), \xi_2(t)$.

By showing that suitable generalized second moments are decreasing
in time it could be proved, that two oriented peaks develop
at two exactly opposite orientations $\tilde{\xi}_1, \tilde{\xi}_2$,

if initially two slightly asymmetric oriented peaks are present.

Their final masses \tilde{m}_1, \tilde{m}_2 can be different.

These initial peaks may differ in size but should both be of higher
order of magnitude in size than the rest of the initial distribution.

So we obtained local stability

for alignment into two opposite directions,

*but **NO** selection of mass.*

[Primi - S. - Velázquez]

Have a closer look at the case $\sigma > 0$.

If the orientational angle V is very small
the kinetic equation can be approximated by

$$\partial_t f = \frac{\sigma^2 m}{2} \partial_{xx} f + \partial_x \left(f(x) \int_I V(x-y) f(y) dy \right)$$

We are interested in the steady states.

An equivalent formulation for these is

$$\begin{aligned} \frac{\sigma^2}{2} \partial_x f(x) + f(x) \int_I V(x-y) f(y) dy &= 0 \\ \int_I f(x) dx &= 1 \text{ and } f(x+1) = f(x) \end{aligned}$$

Heuristics for the Selection Mechanism

Let $\sigma = 0$, then the equation reduces to

$$f(x) \int_I V(x-y)f(y)dy = 0$$

Any function of the form $f(x) = \alpha\delta_0(x) + \beta\delta_0(x - \frac{1}{2})$ is a solution, for arbitrary choice of α, β .

For $\sigma > 0$ this is not the case.

Suppose $f_\sigma \rightarrow \alpha\delta_0(x) + \beta\delta_{\frac{1}{2}}(x)$ for $\sigma \rightarrow 0$.

For $\sigma \ll 1$, f_σ can then be approximated by the solution of

$$\begin{aligned}\frac{\sigma^2}{2}\partial_x f(x) + f(x)V_{\alpha,\beta}(x) &= 0 \\ \int_I f(x)dx &= 1\end{aligned}$$

where $V_{\alpha,\beta} = \alpha V(x) + \beta V(x - \frac{1}{2})$.

This equation can be solved explicitly

$$f(x) = \frac{\exp(-\frac{2}{\sigma^2}[\alpha\phi(x) + \beta\phi(x - \frac{1}{2})])}{\int_I \exp(-\frac{2}{\sigma^2}[\alpha\phi(y) + \beta\phi(y - \frac{1}{2})])dy}$$

with $\phi(x) = \int_0^x V(z)dz$, so $\phi(x) = \phi(-x)$.

Assume $\phi(\frac{1}{2}) \neq 0$, which is generally the case.

The condition for having two peaks concentrated at $x = 0$ and $x = \frac{1}{2}$ is that $\alpha\phi(x) + \beta\phi(x - \frac{1}{2})$ reaches its minimum at these points.

In particular $\alpha\phi(0) + \beta\phi(-\frac{1}{2}) = \alpha\phi(\frac{1}{2}) + \beta\phi(0)$.

This can only happen for $\alpha = \beta = \frac{1}{2}$.

What are the conditions on V for either one or two peaks of equal size to occur?

Suppose for $\sigma \ll 1$ exists a peak-like smooth function f , mainly concentrated at 0, which solves

$$\begin{aligned} \frac{\sigma^2}{2} \partial_x f(x) + f(x) \int_I V(x-y) f(y) dy &= 0 \\ \int_I f(x) dx &= 1 \end{aligned}$$

and converges to δ_0 for $\sigma \rightarrow 0$.

This function may be approximated by the solution of

$$\frac{\sigma^2}{2} \partial_x f(x) + f(x)V(x) = 0, \quad \int_I f(x)dx = 1.$$

Therefore

$$f(x) = \frac{\exp(-\frac{2}{\sigma^2} [\int_0^x V(z)dz])}{\int_I \exp(-\frac{2}{\sigma^2} [\int_0^y V(z)dz])dy}$$

For $\int_0^{\frac{1}{2}} V(x)dx > 0$ we have a main concentration around 0.

For $\int_0^{\frac{1}{2}} V(x)dx < 0$ the peak is located at $\pm \frac{1}{2}$,
which is a contradiction.

Haptotaxis and Trail Following:

We consider a Keller-Segel model with non-diffusive memory, namely

$$\partial_t u = \Delta u - \nabla \cdot (u \nabla \log(v)) \quad , \quad \partial_t v = uv^\lambda \quad .$$

Earlier results:

$\lambda = 0$ global solutions (Chen Hua et al),

$\lambda = 1$ blow-up for specific initial data (Levine and Sleeman).

By setting $\theta = \frac{1}{1-\lambda}$ and $z = \frac{1}{1-\lambda} v^{(1-\lambda)} = \theta v^{\frac{1}{\theta}}$ we obtain

$$\partial_t u = \Delta u - \theta \nabla \cdot (u \nabla \log(z)) \quad , \quad \partial_t z = u \quad , \quad \theta \in (0, \infty)$$

[Kang - S.- Velázquez]:

Space Dimension 1:

For $\theta = 1$, i.e. $\lambda = 0$ formally every space dependent function is asymptotically a steady state for $t \rightarrow \infty$.

It could be shown, that the long time dynamics are strongly dependent on the initial data.

For $1 < \theta < 3$, i.e. $0 < \lambda < \frac{2}{3}$ it was rigorously proved that solutions converge to a Dirac mass for $t \rightarrow \infty$.

Here we only give the heuristic argument:

Assume $I = [-1, 1]$, $\int_I u dx = m$ and consider

$$\bar{z}_t = \frac{\bar{z}^\theta}{\int_I \bar{z}^\theta dx},$$

which results from the quasisteady approximation

$$\begin{aligned} 0 &= \nabla \cdot (\nabla u - \theta u \nabla \log(z)) \\ \partial_t z &= u \end{aligned}$$

We assume that this is a good approximation for the original problem for $t \rightarrow \infty$.

For $\bar{z}(0, 0) > \bar{z}(0, x)$ we obtain

$$\bar{z}^{1-\theta}(t, x) = \bar{z}^{1-\theta}(0, x) - (\theta - 1) \int_0^t \frac{ds}{\int_I \bar{z}^\theta(s, x) dx}$$

Assume the following expansion:

$$\bar{z}^{1-\theta}(0, x) = \bar{z}^{1-\theta}(0, 0) + Bx^2 + h.o.t. \text{ for } x \rightarrow 0.$$

$$\text{Thus } \bar{z}^{1-\theta}(t, x) \approx \bar{z}^{1-\theta}(0, 0) + Bx^2 - (\theta - 1) \int_0^t \frac{ds}{\int_I \bar{z}^\theta(s, x) dx}.$$

So $\bar{z}^{1-\theta}(t, x) \approx Bx^2 + \psi(t)$, and

$$\text{therefore } \bar{z}(t, x) \approx (Bx^2 + \psi(t))^{\frac{1}{1-\theta}}.$$

Explicit calculations show that

$$\frac{1-\theta}{\psi'(t)} \approx \int_I \frac{dx}{(Bx^2 + \psi(t))^{\frac{\theta}{\theta-1}}}, \text{ and}$$

$$\psi'(t) \approx -K \psi^{\frac{\theta+1}{2(\theta-1)}}(t), \text{ so } \psi(t) \approx At^{\frac{2(1-\theta)}{3-\theta}}.$$

With this we can calculate, that

$$\bar{z}(t, x) \approx \frac{t^{\frac{2}{3-\theta}}}{\left(Bx^2 t^{\frac{2(\theta-1)}{3-\theta}} + A \right)^{\frac{1}{\theta-1}}}$$

Theorem:

There exist initial data $(u_0, z_0) \in C^{2,\alpha}$ such that the corresponding solutions (u, z) of our system satisfy $u(t, x) \rightarrow m\delta(x)$ and

$$\bar{z}(t, x) \approx \frac{t^{\frac{2}{3-\theta}}}{\left(Bx^2t^{\frac{2(\theta-1)}{3-\theta}} + A\right)^{\frac{1}{\theta-1}}}$$

for $t \rightarrow \infty$, and where A, B are constants, which depend on the initial data.

Consider again

$$\begin{aligned}\partial_t u &= \Delta u - \nabla \cdot \left(u \frac{\nabla v}{v} \right) \\ \partial_t v &= uv^\lambda\end{aligned}$$

for $x \in \mathbb{R}^n$, $t > 0$, and suitable initial conditions for u and v .

Depending on the space dimension n , the growth exponent λ and the regularity properties of the initial conditions, blow-up in finite time, mass aggregation in infinite time, or mass spreading can be observed.

1 Intuitive Understanding of the Model in \mathbb{R}^d

The exponent λ measures the strength of the localized reinforcement, thus the tendency for aggregation increases with larger values of λ , respectively larger values of θ .

The dynamics of the cells are described by random motility and by chemotactic drift towards higher concentrations of v .

The number of times that a brownian particle approaches a given point in space depends very strongly on the space dimension.

Thus the environment, where the cells move, is modified stronger in lower dimensions than it is in higher dimensions. So in this model the tendency to aggregate increases for smaller spatial dimension.

In contrast to this, in the original Keller-Segel model with diffusion finite time blow-up is more likely in higher dimensions.

Regular initial data, $n = 1$:

The reinforced random walk in one dimension suggests $\lambda = 0$ as critical parameter.

- For $\lambda > \frac{2}{3}$ we observe blow-up in finite time.
- For $0 < \lambda < \frac{2}{3}$ we observe blow-up in infinite time.
The rate of growth is a power law.
- For $\lambda = \frac{2}{3}$ also blow-up in infinite time can be observed.
The rate of growth is exponential.
- For $\lambda = 0$ the solution is highly sensitive on the initial data.
These play an important role for the diffusive tails of the solution.
- For $\lambda < 0$ self-similar behavior can be observed.
The reinforcement plays a non-trivial role.
The solution behaves non-diffusive.

In [S. '95], [Othmer - S., '97] the following limiting systems were formally derived from self-reinforced, attractive random walk models:

a) edge reinforcement:

$$\begin{aligned}\partial_t u &= \nabla \cdot (\nabla u - u \nabla \log v) \\ \partial_t v &= f(u, v) = uv^\lambda\end{aligned}$$

b) vertex reinforcement:

$$\begin{aligned}\partial_t u &= \nabla \cdot (\nabla u - 2u \nabla \log v) \\ \partial_t v &= f(u, v) = uv^\lambda\end{aligned}$$

For $\theta = \frac{1}{1-\lambda}$ and $z = \frac{1}{1-\lambda}v^{(1-\lambda)} = \theta v^{\frac{1}{\theta}}$ we have

$$\begin{aligned}\partial_t u &= \nabla \cdot (\nabla u - \theta(u \nabla \log(z))) \\ \partial_t z &= u, \quad \theta \in (0, \infty)\end{aligned}$$

If $\theta = \theta_e$ then the formal limit of vertex reinforcement gives

$$\theta_v = \frac{2}{(1-\lambda)} = 2\theta.$$

So $\frac{1}{2}\theta_v = \theta_e$ shows the same equation/effect.

Though the asymptotics of the corresponding integro-differential-equation do **not** coincide with the asymptotics of the discrete random walk, the integro-differential-equation correctly predicts/recovers the critical θ for which the behavior for the cell/particle switches from visiting all integers infinitely often to being trapped in a finite number of integers.

The approximation recovers and predicts the following:

1-dim edge reinforcement:

$\theta_e > 1$: trapping in two points (Davis)

$\theta_e = 1$: trapping in a bounded region (Merkl - Rolles)

$\theta_e < 1$: spreading dominated by boundary layers (Toth)

1-dim vertex reinforcement:

$\theta_v = 1$: trapping in 5 points (Tarres)

$\theta_v = \frac{1}{2}$: critical case

$\frac{1}{2} < \theta_v < 1$: trapping in many points

Interestingly (*compare the PDE relation between θ_v and θ_e*) for the discrete $\theta_e \in (0, 1)$ and the discrete $\theta_v \in (0, \frac{1}{2})$, both below their respective critical value, the asymptotic behavior of the discrete $z_v(\theta)$ ‘coincides’ with that of $z_e(\frac{\theta}{2})$.

Similar asymptotics are done for the higher dimensional cases, in order to make educated guesses about the behavior of the respective self-attracting random walk.

- The classical Keller-Segel system for chemotaxis behaves in a different way than the PDE-ODE-system presented. The later one behaves ‘more hyperbolic’. The reaction to an attractive but localized signal creates a different long time behavior if compared to attractive diffusible signals.
- Edge and vertex reinforcement make a difference in the one particle setting, but in certain parameter regimes they behave surprisingly similar. The PDE-ODE-model astonishingly gave hints for the critical parameter but does not provide the right asymptotics. The critical parameter seems to be very robust w.r.t. approximations.